Exploration of the Townsend regime by discharge light emission in a gas discharge device*

Hilal Yucel Kurt†

Gazi University, Faculty of Sciences, Department of Physics, 06500 *Ankara, Turkey*

(Received 8 March 2013; revised manuscript received 18 April 2013; published 3 December 2013)

The Townsend discharge mechanism has been explored in a planar microelectronic gas discharge device (MGDD) with different applied voltages U and interelectrode distance d under various pressures in air. The anode and the cathode of the MGDD are formed by a transparent SnO_2 covered glass and a GaAs semiconductor, respectively. In the experiments, the discharge is found to be unstable just below the breakdown voltage U_b, whereas the discharge passes through a homogeneous stable Townsend mode beyond the breakdown voltage. The measurements are made by an electrical circuit and a CCD camera by recording the currents and light emission (LE) intensities. The intensity profiles, which are converted from the 3D light emission images along the semiconductor diameter, have been analysed for different system parameters. Different instantaneous conductivity σ_t regimes are found below and beyond the Townsend region. These regimes govern the current and spatio-temporal LE stabilities in the plasma system. It has been proven that the stable LE region increases up to 550 Torr as a function of pressure for small d. If the active area of the semiconductor becomes larger and the interlectrode distance d becomes smaller, the stable LE region stays nearly constant with pressure.

Keywords: Townsend discharge, breakdown, microelectronic gas discharge device, semiconductor cathode

PACS: 52.80.Dy, 52.77.–j, 73.61.Ey **DOI:** 10.1088/1674-1056/23/1/015201

1. Introduction

Gas discharge plasmas are widely used in many technological applications, such as plasma display panels, light emiting systems, displays, lasers, atmospheric plasma units, fusion, surface treatments and the sterilization of biological samples.[1–8] In addition, surface etching and deposition processes of thin film layers in the semiconductor industry, protective coating in analytical chemistry, biotechnological and environmental applications also include discharge plasmas to manufacture the desired products.[9,10] Gas discharge devices with semiconductor electrodes have usually been used to convert infrared (IR) signals into visible images.[11–15] In the above applications, the interactions of the materials, namely, semiconductors, metals, polymers and dielectrics with gas discharge, cause some differences in their ordinary features because of the surface modification.[16] It has also been known that any change in the emission of electron features of cathodes under the discharge may be undesirable and yield some spatio–temporal instabilities as functions of the system parameters.[16]

There are two modes for the discharge, namely, Townsend and glow discharges.[17] The Townsend discharge is a very weak discharge with a low space charge production (i.e., current). Liang *et al.*[18] also proved that since the space charge produced by the Townsend discharge is too small to deteriorate the electric field inside the gas gap, the electrons have the same energy over the entire gap on average and therefore, the spatial distribution of the discharge light becomes proportional to the distribution of the electron density. Thereby, the applied uniform electric field cannot be detoriated. In this case, the maximal light emission (LE) from the excited atoms in the media is observed around the anode.[19,20] Different from the Townsend discharge, a stronger discharge with a higher space charge production occurs in the case of a glow discharge.[21] Strictly speaking, a swarm of positive space charge accumulates near the cathode forming a cathode fall. This is observed as a highly luminous layer close to the cathode. The Townsend discharge is ignited at very low currents when any discharge system is connected to a high-voltage direct-current (dc) power supply through a sufficiently large resistance.[22] Since the Townsend discharge is a complex phenomenon, discharge gap d, electrode geometry, filled gas type and pressure all play important roles in characterizing the discharge. In most of the studies,[22,23] it was found that the applied voltage is almost indistinguishable from the breakdown voltage U_b. However, in a typical Townsend breakdown, the electric field and the ion density are almost uniformly distributed along the gap.[24] A large number of initial electrons create a current before the breakdown[25] and the electrons can be produced via the associative ionization,[26] desorption of electrons from the barriers,[27] or electron emission by metastable species.[28] It is known that the Townsend regime is limited to a small discharge range. In addition, the discharge turns to a filamentary state with the increase in the interelectrode distance d.[25] In fact, this filamentary state may occur at higher frequencies or applied voltages U.[25] Both theoretical and experimental find-

*Project supported by Gazi University BAP Research Project, Turkey (Grant Nos. 05/2012-47 and 05/2012-72).

†Corresponding author. E-mail: hyucelkurt@gmail.com

© 2014 Chinese Physical Society and IOP Publishing Ltd

ings prove that the applied voltage U, which enables the production of a current between the electrodes, is the breakdown voltage U_b and the Paschen curve can be obtained as a function of the multiplication of pressure p and d.[25,29,30]

If one of the electrodes is manufactured from a semiconductor with high resistivity, a stable Townsend discharge is obtained in a microelectronic gas discharge device (MGDD).[6,31] The discharge instabilities leading to current filamentation in the MGDD are dominated by the local negative feedback because of the voltage drop on the semiconductor electrode.[13,32] Since the ion concentration in the discharge gap is too small to create an important distortion on the electric field even at a high current density, a spatially homogeneous state of Townsend discharge is observed in the system for a wide range of p.[6,33] While the coherent current oscillations are obtained over the whole range of parameters and current in the case of metallic electrodes, the distance between the electrodes suppresses the oscillations and causes a dc mode in a certain range of current in the semiconductor electrode. Thus, when d is decreased, the range of current expands and the coherent oscillations may disappear.

In this paper, the Townsend discharge mechanism is explored in an air filled MGDD and the effects of the system parameters are reported. In Section 2, experimental details and the setup are presented. The main results and discussion are given in Section 4. Finally, the concluding remarks are given in the last section.

2. Experiment

The complete setup of the MGDD is shown in Fig. 1(a). The main part, the discharge cell, is denoted by No. 4 (Figs. 1(a)–1(c)), where a GaAs semiconductor is situated at the cathode part of the cell. From the right to the left, the total testing system consists of an external light source, an optical lens for visible light emitted from the source, a silicon filter, a discharge cell, a CCD camera, a vacuum pump, a vacuum valve, a facility box and a digital manometer. A detailed schematic diagram of the overall setup is shown as a sandwich-like cell with the measurement and recording facilities (Fig. 1(b)). The gas-discharge gap is situated between two electrodes: one of them is an SnO_2-covered glass layer and the other one is made of a semiconductor (i.e., GaAs). The gap can be adjusted by spacers of different thicknesses from 45 μm to 323 μm.

The discharge light emission (DLE) recorded by the CCD camera (ITIIC equipped with a proximity focused Gen II image intensifier coupled to the charge coupled device via a tapered fiber optic) is conveyed to a PC as shown in Fig. 1(b). In order to measure the electrical features of the DLE, a PC and some interface devices are used to record the current–voltage characteristics (i.e., CVC) of an individual DLE in addition to the DLE patterns of GaAs. The electrical current I flowing through the cell and the voltage U over the cell are measured synchronously by a Keithley 199 multimeter and a Stanford PS 325 type voltage supply. These measurements are digitalized via home-made software.

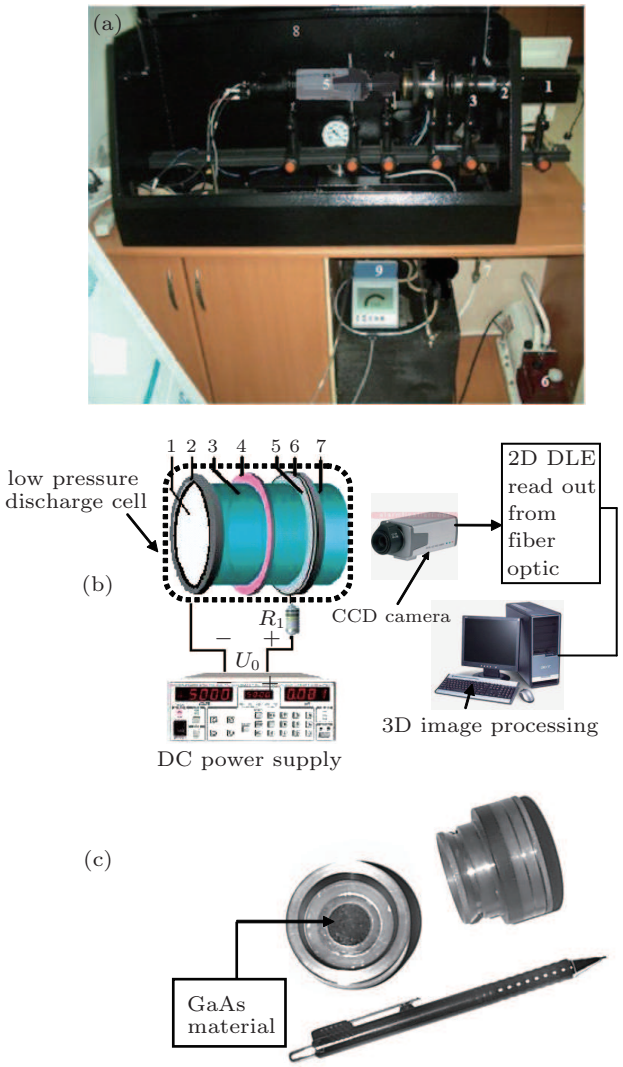


Fig. 1. (color online) (a) Photo of MGDD: 1: light source; 2: optical lense; 3: silicon filter; 4: gas ionization system (IS); 5: CCD camera; 6: vacuum pump; 7: vacuum valve; 8: facility box; and 9: digital manometer. (b) Sketch of a sandwich-like ionisation cell, the measurement and recording devices: 1: GaAs material; 2: specimen holder; 3: microdischarge gap of the cell; 4: insulator mica; 5: transparent conductor (SnO_2); 6: glass disc; and 7: visible light beam. The dashed part in panel (b) is shown in panel (c). The GaAs material is at the middle of the cell. Interelectrode distance d (in μm) is the distance between GaAs material and transparent SnO_2 conductor.

The CVCs are recorded for different voltages within a rate of 5 V·s^{-1}. Current I is measured by finding the voltage on a load resistance of 10 kΩ, which is attached to the cell. The stability of the gas discharge is explored by using the set-up with an interelectronic distance d. The DLE can be obtained by a photon counting mechanism, ELSEC 9010 from Littlemore Sci. Eng. In the case of optical excitation of the GaAs sample, the gas system can be operated under different IR light in order to excite the electronic states of the GaAs samples. The

external light source is used for the optoelectrical exploration of the MGDD. In that case, the photocathode can be uniformly illuminated by an incandescent lamp of 250 W in front of the cathode. Therefore, the photoconductivity of the sample can be increased up to a certain level. The illumination intensity L_n can be varied between 10^{-6} W·cm^{-2} and 10^{-2} W·cm^{-2} by the use of filters. Between the incandescent lamp and the sample, there exists a Si filter, which transmits light of the wavelengths between 0.9 μm and 1.6 μm. The maximum illumination is measured as 8×10^{-2} W·cm^{-2}. Besides, the experiments can also be performed in the dark by exploring the plasma discharge structures in the cell. The experiments can be performed in the pressure range of 15–690 Torr for the discharge cell. The voltage applied to the discharge cell can be gradually increased from 200 V to 2.5 kV to study the responses of the GaAs cathode and plasma media under different discharge conditions. In gas discharge studies, the surface of GaAs (1 0 0) is used as the cathode.[34] It should be noted that the DLE patterns can be recorded via the CCD camera successively when the applied voltage U is increased step by step. In addition, a constant U can also be used during a certain duration to obtain a detailed DLE for the 3D processing. Following the record of the 2D DLE patterns, which are received by the CCD camera, the patterns are sent to the PC. Then the 3D patterns are created by a software package (Image pro Plus)[35] and are digitalized by the gray numbers over the entire DLE surface for the spatial identification of the discharge regime. The experiments are conducted around the gas discharge current density $j = 50$ μA·cm^{-2}. In order to ascertain the current density of plasma media or to seek the behavior at different current densities, various light illumination intensities (L_1, L_2 and L_3) can be used in the set-up. In fact, such low j values guarantee a Townsend-mode discharge regime.[34,36] Because this value is lower than the critical current rates observed in the transitions from Townsend to glow regimes.

3. Background on breakdown

A breakdown curve is defined as the threshold of a transition from a non-conductive medium into a conductive one inside the plasma when a sufficiently strong electric field is applied. In this manner, the relation between the creation and annihilation of the electrons determines the breakdown threshold.[13] The applied voltage causing a transition from a non-self-sustaining discharge to a self-sustaining discharge has been known as the breakdown voltage. The breakdown is then determined by a rapid gas transition from a poor electrical conduction with high resistivity (about 10^{14} Ω·m) to a relatively good conduction with lower resistivity.[37] Inside a plasma medium, the time lag of a breakdown is given by the sum of the retardation time and the formative time. The retardation time is dependent on the probability to get primary electrons for starting the carrier multiplication. In fact, it is a statistical concept having the typical values at the order of 10^{-5} s or 10^{-3} s. The retardation time is also affected by the discharge geometry. For instance, it can be nearly a hundred times longer in very narrow gaps compared to that in the wide gaps with the same p. On the other hand, the formative time is the effective time to buildup an electrical current inside the plasma structure. It usually has values around 10^{-8}–10^{-4} s with regard to the plasma processes of electron multiplication.[38] According to the Townsend breakdown theory, the carriers are generated depending on the ionization coefficient α and the secondary emission coefficient γ. At the right-hand side of the Paschen curve (i.e., higher p), the breakdown voltage increases almost proportionally with the product of d and p. Because the possibilities for the ionization collisions are too limited and a very strong field is required to achieve the necessary amplification, thereby, the breakdown voltage exhibits a minimum where the ionizing capability of electrons is at maximum. Due to these two conditions, the minimal voltage for the breakdown is most favorable, since the plasma media for the above-mentioned multiplications are optimal.

4. Results and discussion

Figure 2(a) shows the breakdown curves for different diameters of the GaAs cathode. From Fig. 2(a), it is obvious that the minimum point of the discharge skips up to higher pressures when a larger GaAs diameter is used at the cathode. This reality is reasonable since the surface charge plays an important role to identify the Paschen curve as stated above. In addition, the breakdown voltage for the optimal discharge gets lower from 360 V to 340 V due to the surface charge effects. It should be also noted that the inclination of the curve decreases in the case of large GaAs cathodes. Therefore, an easier discharge is achieved at larger pressures compared to the cases with small GaAs cathodes. According to the findings in Refs. [39] and [40], as seen in Fig. 2(a), the metallic cathode can give a broader region in comparison with the semiconductor cathode. However, the general trends of the curves are similar. Since the cathodes are conducting materials in the studies of Refs. [39] and [40], the breakdown voltages at larger p become lower in comparison to that with the semiconducting cathode.

Figure 2(b) shows the differences of successive U_B values in Fig. 2(a). This graph is very useful to identify the pd values, where the minimum breakdown point sits. This reality comes from the fact that the inclination of the breakdown curve becomes zero at its lowest part of the mathematical information. In fact, this graph assists in indicating the difference of U_B (i.e., ΔU_B) and one can clearly identify the minimal point of the Pacshen curve. For instance, $pd = 1.6$ Torr·mm and $pd = 3$ Torr·mm can be understood easily for $D = 12$ mm and $D = 22$ mm, respectively, by looking at the x-axis values where $\Delta U_B = 0$. These points correspond to the values of the differentiation of U_B equals to zero. In addition to the determination of minimal points, Fig. 2(b) also gives an idea of the

inclination of the right branches. For instance, while the averaged difference of the right branch at $D = 12$ mm (red) is found to be 30 V, the averaged difference of the other plot at $D = 22$ mm (black) is found to be 20 V.

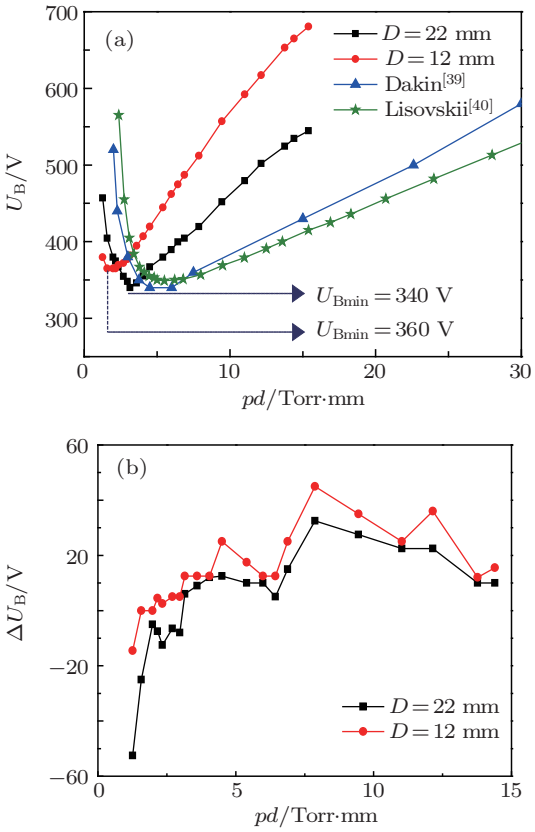


Fig. 2. (color online) (a) The breakdown curves: two curves are measured from the GaAs cathode with different diameters and the other two are taken from the studies in Refs. [39] and [40] for comparison. (b) The differences of U_B from the GaAs cathode with respect to p.

In order to show the system reply for the voltage changes, Fig. 3 is drawn. While the upward (red) direction indicates the reply as an increasing current, the downward (blue) direction gives the reply as a decreasing current. The interesting behavior is that the upward and downward curves follow the same path. Strictly speaking, some experimental results indicate hysteresis phenomena for special values of d and p.[41,42] This kind of hysteresis effect occurs for large d values and low pressures according to our previous studies and it is believed that the charged particles can have two different energy states. According to our recent studies,[40,41] a lower p, such as 44 Torr, and a larger d, such as 445 μm, give a hysteresis behavior. For more detailed expressions, readers are referred to Refs. [41] and [42]. In that case, one expects that some amount of energy is given to the plasma and that the energy is proportional to the area of the hysteresis loop.[42,43] However, we have not observed any hysteresis effect for this explored parameter range. This situation is known as the reproducibility and it results with a very stable current–voltage characteristic, which is important for the technological manufacturing. According to Fig. 3, the plasma resistivity or conductivity changes with U. In fact, five different regions exist in the plot. Before the breakdown, the resistivity of the plasma is the highest. Then the resistivity becomes much lower just after the breakdown. Then a moderate resistivity region occurs between 660 V and 835 V. After this regime, another lower resistivity region is observed for a very short voltage range (i.e., nearly 20 V) and the moderate resistivity region persists for relatively higher voltages.

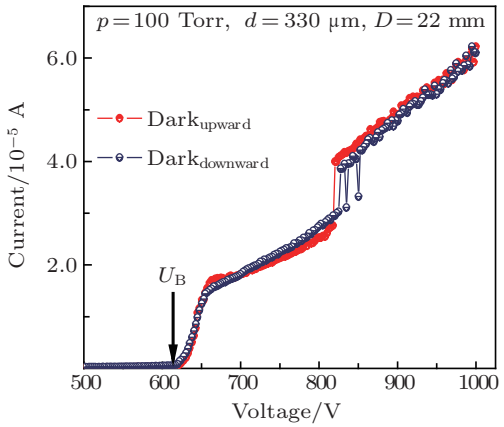


Fig. 3. (color online) The step up/down condition of the semiconductor-plasma micro structure in the Towsend regime.

Figure 4 shows the 2D and 3D discharge patterns from the measurements via the CCD camera. It is shown that the records of 2D, 3D discharge images and profiles through the semitransparent SnO_2 anode provide valuable information on the kinetics of the breakdown. The discharge passes from the non-self-sustained unstable discharge to the Townsend regime from $U = 340$ V to $U = 780$ V. When the voltage reaches the breakdown value as shown in Fig. 4(a), the optical appearance of the pattern is not spatially smooth. In fact, the profile in Fig. 4(a) has an unstable appearance with high and low intensity peaks. However, when the applied voltage is further increased, the pattern is much more homogeneous, as shown in Figs. 4(b) and 4(c), and the DLE becomes relatively homogeneous, spreading to the entire active area of the cathode.[35] This situation is much more observable in the corresponding profiles. In fact, a better pattern is obtained at $U = 780$ V. In the Townsend mode, large numbers of electrons are produced with the increasing voltage, as also seen in Ref. [16]. The maximum electron density is observed near the anode and it radiates the corresponding DLE in this mode. As a result of the high electron production, photoemission and photoionization cause a homogeneous image on the entire cathode surface. The DLE profiles at the right-hand sides of the patterns give a better explanation for the homogeneity of the patterns. While the DLE difference between the maximum and the minimum is 140 arb. units at $U = 340$ V, it drops to 5 arb. units at $U = 780$ V by giving a much smoother emission surface.

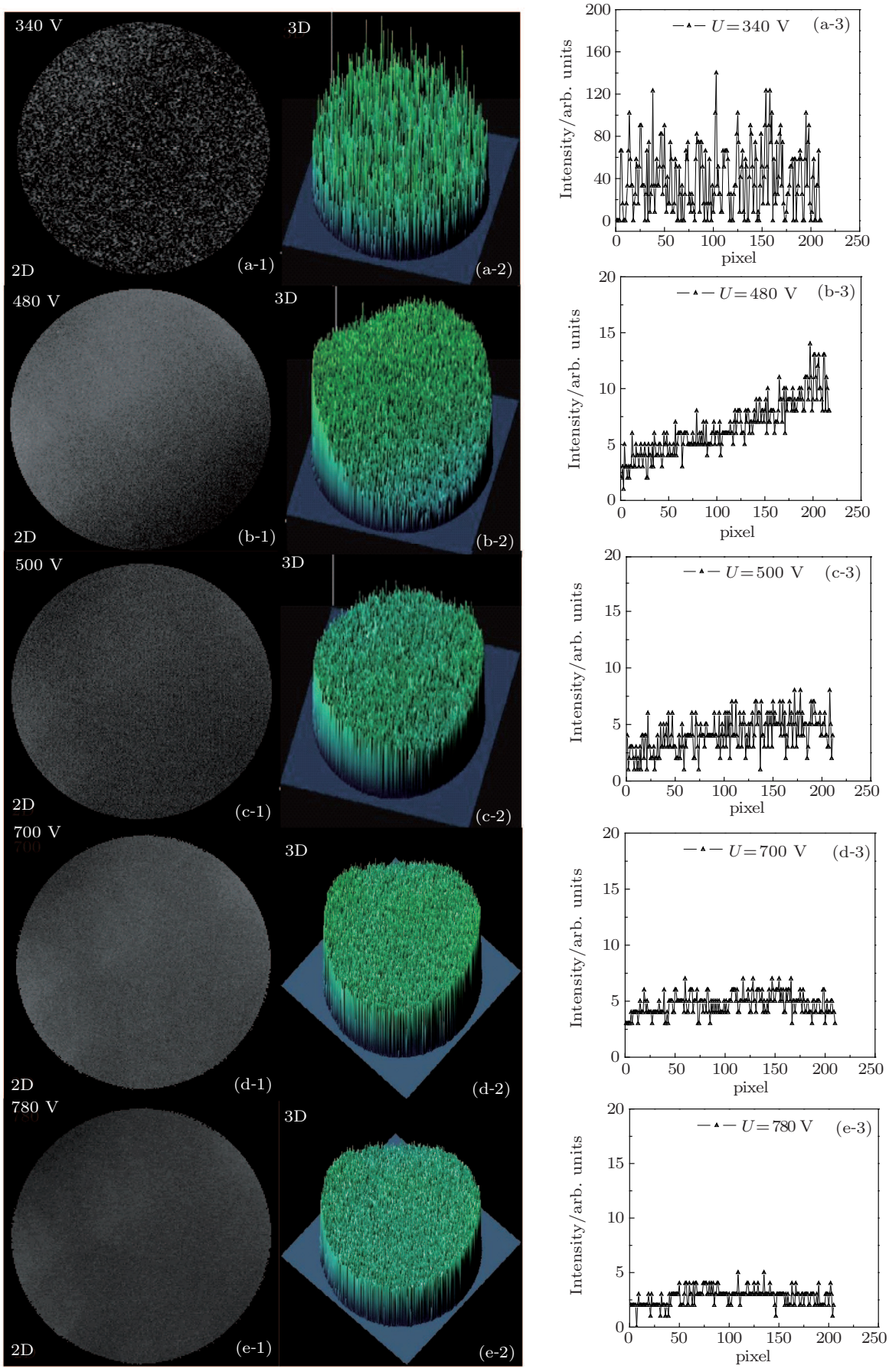


Fig. 4. (color online) DLE intensities at different U ((a)–(e)) in the breakdown and Townsend regimes. System parameters are $d = 45$ μm, $D = 22$ mm, and $p = 100$ Torr.

Figure 5 shows the current versus time for different applied voltages. It is obvious that a bistable fluctuation exists at $U = 340$ V, which corresponds to the region below the Townsend regime. When the voltage increases, the curves exhibit more stable behaviors parallel to the corresponding DLE patterns in Fig. 4. The current becomes more stable with decreasing fluctuation at $U = 780$ V. It can be stated that the optimal voltage is 780 V for the suitable operation of the system. With regard to the oscillations for 500–600 V, it can be stated that a time lag between the ion formation near the anode and the enhancement of the current due to the ion-electron emission occurs in the system.[31,32] In addition to this ion-electron emission, the origin of oscillations can also be accepted as a result of the space charge. Strictly speaking, the space charge of ions distorts the electric field and changes the multiplication coefficient for electrons. For higher U values, a more stable current waveform has been measured due to the electron abundancy, which decreases the space charge effect.

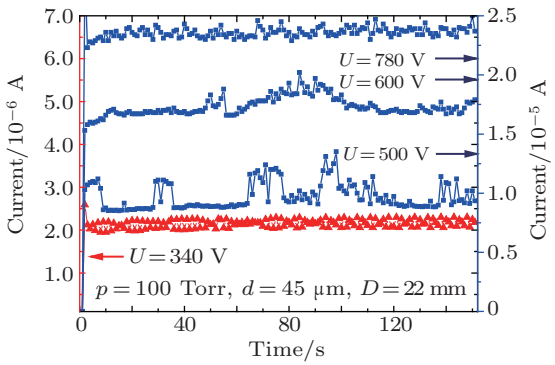


Fig. 5. (color online) Current variation with respect to time for different applied voltages. The red plot corresponds to an unstable pre-Towsend regime, the blue plots correspond to the Townsend regime.

The measured instantaneous plasma conductivity of the system is presented in Fig. 6 as a function of time. While the conductivity changes suddenly at $U = 340$ V due to the unstable behavior at the pre-Townsend region, one gets temporally smooth conductivity at higher voltages. Due to the complexity in the plasma medium, these types of instant changes occur in conductivity. However, the Townsend regime has smoother conductivity. The instantaneous conductivity is found from the formulation $\sigma(t) = \Delta I(t)d/US$, where $\Delta I(t)$is the successive difference in current measurements and d, U and S are the interelectrode distance, the applied voltage and the active cross sectional area of the gas discharge cell, respectively. It is obvious that the instantaneous conductivity can reach up to $10^{-6}\ \Omega^{-1}\cdot\mathrm{cm}^{-1}$ and have negative instantaneous values temporally in the complicated plasma media. The plasma conductivity slightly decreases at a higher voltage (i.e., $U = 480$ V) and has a value of $5 \times 10^{-7}\ \Omega^{-1}\cdot\mathrm{cm}^{-1}$. However, the fluctuations appearently decrease at the Townsend regime compared to the unstable non-self-sustaining discharge.

Figure 7 gives the DLE for different system parameters. It is measured by using a photon counting mechanism under wide ranges of system parameters. While Fig. 7(a) presents the largest DLE region for a small interelectrode distance d and a large semiconductor diameter D, the intensities become smaller for larger d and smaller D, as shown in Fig. 7(c). Smaller DLE intensities are observed at $d = 323$ μm and $D = 9$ mm. These plots are also important to find the optimal emission regions of the system. According to the measurements, a small interelectrode distance and a large diameter semiconductor should be used for obtaining a larger stable emission region. In this case, the system emits light between 28 Torr and 550 Torr. However, the stable DLE region becomes smaller for $d = 323$ μm and $D = 9$ mm and it survives between 28 Torr and 220 Torr. Note also that the produced maximal emission exceeds the photomultiplier limits (i.e., 5 arb. units) in Figs. 7(a) and 7(b), therefore they are cut above. According to Fig. 7, it is interesting that the system can produce light emission at higher pressures up to 600 Torr when $d = 45$ μm and $D = 18$ mm are used. Therefore, narrow interelectrode gaps should be preferred for high pressurized discharge cells in order to have better light emission.

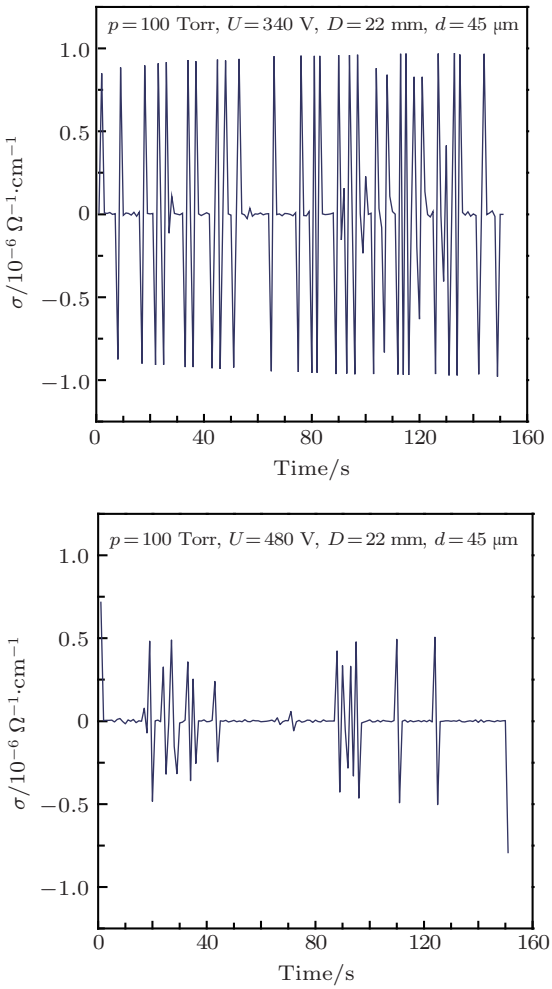


Fig. 6. (color online) Measured instantaneous conductivities of the MGDD at (a) $U = 340$ V and (b) $U = 480$ V.

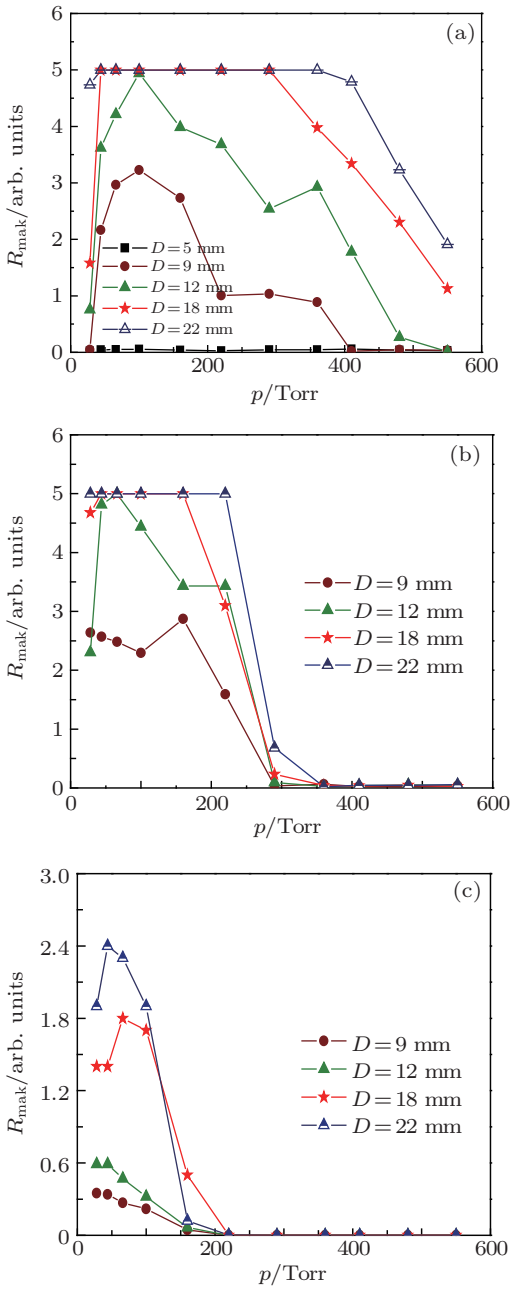


Fig. 7. (color online) Maximum DLE values for different diameters D and interelectrode distances d ((a) $d = 45$ μm, (b) $d = 143$ μm, (c) $d = 323$ μm). The applied voltage is $U = 780$ V.

The DLE intensities for different diameters of the semiconductor cathode are shown in Fig. 8. Note that this 3D graph gives the emissions for external illuminations including the dark regime. While L_1 denotes the moderate external illumination intensity from the cathode side of the discharge cell, L_2 has the maximal external intensity. The illuminations are given in the IR region as stated in the experimental section. Therefore, it is proved that the conductivity rate of the semiconductor has been increased by the photon absorption. As shown in Fig. 8, the intensity increases by the increase of the active area in the semiconductor cathode since the carriers in the semiconductor increase relatively.

However, L_1 and L_2 illuminations cause dramatic enhancements in emission, as shown in Fig. 8. Since the photomultiplier sensitivity is only up to 5 arb. units, the upper parts of the emissions are cut. On the other hand, D also plays an important role in increasing the emission intensity from the system; it can be comparable with the change made by the external illuminations L_1 and L_2. In addition, these emission patterns prove that two maximal intensity peaks appear at high D and high illumination intensities, as observed at $D = 22$ mm for different pressure rates. It can be concluded that the maximal intensities obtained from the MGDD result from the complicated combination of pressure, external IR illumination, D and d. Strictly speaking, the optimal parameters for the maximal DLE intensity are found to be $(D, d, L_n) = (22, 45, L_2)$. These results prove that the complicated plasma structure depends on the physical parameters of the gas discharge device, such as D, p and illumination.

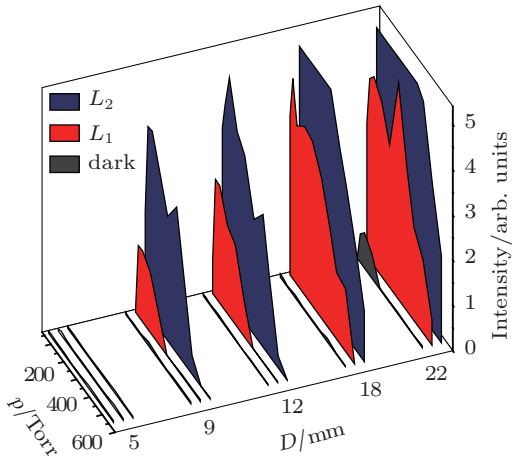


Fig. 8. (color online) DLE intensities for different external illumination intensities. The interelectrode distance is $d = 45$ μm.

5. Conclusion

The discharge event in an MGDD is found to be very complicated in terms of the pressure, interelectrode distance, applied voltage and active area of the semiconductor GaAs. The system is found to be unstable at the pre-Townsend regime where relatively lower voltages are applied. There exists no smooth discharge pattern at this regime. However, the DLE patterns become more homogeneous at the Townsend regime, since the electrons move more easily from the semiconductor to the anode. The optimal parameters for the maximal DLE intensitiy are found to be $(D, d, L_n) = (22, 45, L_2)$. The instantaneous plasma conductivity becomes more stable with respect to time in the Townsend region. There also exist very low conductivities for some time durations. In addition, this work proves that the active area of the semiconductor is as important as the external IR illumination intensities in terms of the formation of the DLE patterns. For larger active areas (i.e., diameter D), two maximal DLE intensities are formed for two different pressure rates, one of which is at a lower pressure, such as 100 Torr, while the other is at a relatively higher pressure, such as 290 Torr. In conclusion, the dynamics of an

MGDD system are very complicated and depends on many parameters including cathode diameters, interelectrode distance and illumination in the Townsend regime.

Acknowledgment

The author thanks Prof. B. G. Salamov for his fruitful suggestions.

References

[1] Portsel L M, Lodygin A N and Astrov Yu A 2009 *J. Phys. D: Appl. Phys.* **42** 235208
[2] Kogelschatz U 2003 *Plasma Chem. Plasma Process.* **23** 1
[3] Park S J and Eden J G 2002 *Appl. Phys. Lett.* **81** 4127
[4] Ouyang J T, Duan X X, Xu S W and He F 2012 *Chin. Phys. Lett.* **29** 025201
[5] Xuechen L, Dongying N, Zengqian Y, Tongzhen F and Long W 2012 *Phys. Plasmas* **19** 083505
[6] Kurt E and Serdal A 2012 *Energ. Convers. Manage.* **63** 55
[7] Li X C, Dong L F and Wang L 2005 *Chin. Phys.* **14** 1418
[8] Mu X D, Mu Z X, Wang C, Jia L and Dong C 2011 *Acta Phys. Sin.* **60** 015204 (in Chinese)
[9] Grill A 1994 *Cold Plasma in Materials Fabrication: from Fundamentals to Applications* (New York: IEEE Press)
[10] Lieberman M A and Lichtenberg A J 1994 *Principles of Plasma Discharges and Materials Processing* (2nd edn.) (New York: Wiley)
[11] Lodygin A N, Portsel L M and Astrov Y A 2012 *Contrib. Plasma Phys.* **52** 682
[12] Portsel L M, Astrov Yu A, Reimann I, Ammelt E and Purwins H G 1999 *J. Appl. Phys.* **85** 3960
[13] Fillard J 1988 *Rev. Phys. Appl.* **23** 765
[14] Kurt H Y, Sadiq Y and Salamov B G 2008 *Phys. Status. Solidi. A* **205** 321
[15] Salamov B G and Kurt H Y 2005 *J. Phys. D: Appl. Phys.* **38** 682
[16] Gurevich L, Kittel S, Hergenroder R, Astrov Yu A, Portsel L M, Lodygin A N, Tolmachev V A and Ankudinov A V 2010 *J. Phys. D: Appl. Phys.* **43** 275302
[17] Raizer Yu P 1991 *Gas Discharge Physics* (Berlin: Springer)
[18] Liang Z, Luo H Y, Wang X X, Bo L V, Guang Z C and Wang L M 2008 *Chin. Phys. Lett.* **25** 2136
[19] Luo H, Liang Z, Lv B, Wang X, Guan Z and Wang L 2007 *Appl. Phys. Lett.* **91** 221504
[20] Petrovic Z L and Phelps A V 1997 *Phys. Rev. E* **56** 5920
[21] Haiyun L, Zhuo L, Xinxin W, Zhicheng G and Liming W 2010 *J. Phys. D: Appl. Phys.* **43** 155201
[22] Mokrov M S and Raizer Yu P 2008 *Plasma Sources Sci. Technol.* **17** 035031
[23] Kurt H Y, Inalöz A and Salamov B G 2010 *Optoelectronics and Advanced Materials - Rapid Communications* **4** 205
[24] Li X C, Niu D Y, Xu L F, Jia P Y and Chang Y Y 2012 *Chin. Phys. B* **21** 075204
[25] Golubovskii Yu B, Maiorov V A, Li P and Lindmayer M 2006 *J. Phys. D: Appl. Phys.* **39** 1574
[26] Segur P and Massines F 2000 *13th Int. Conf. on Gas Discharges and Their Applications*, September 3–8, 2000, Glasgow, UK, p. 15
[27] Golubovskii Yu B, Maiorov V A, Behnke J and Behnke J F 2002 *J. Phys. D: Appl. Phys.* **35** 751
[28] Gherardi N, Croquesel E, Naude N, Veis P and Massines F 2002 *Proc. 8th Int. Symp. on High Pressure Low Temperature Plasma Chemistry* (HAKONE VIII), July 21–25, 2001, Puhajarve, Estonia
[29] Kurt E, Kurt H and Bayhan U 2009 *Cent. Eur. J. Phys.* **7** 123
[30] Golubovskii Yu B, Maiorov V A, Behnke J and Behnke J F 2003 *J. Phys. D: Appl. Phys.* **36** 39
[31] Kurt H, Koc E and Salamov B G 2010 *IEEE Transaction on Plasma Science* **38** 137
[32] Asinovski E I, Kirillin AV and Rakovets A A 1988 *Cryogenic Discharges* (Moscow: Nauka) (in Russian)
[33] Portsel L M, Astrov Yu A, Reimann I and Purwins H G 1997 *J. Appl. Phys.* **81** 1077
[34] Kurt H, Cetin S and Salamov B G 2011 *IEEE Transaction on Plasma Science* **39** 1086
[35] Kıymaz S 2001 *Kızılötesi Görüntü Çeviricideki Elektrot Yüzeylerinin İcelenmesi* (Master Dissertation) (Ankara: Gazi University Institute of Science and Technology) (in Turkish)
[36] Portsel L M, Lodygin A N and Astrov Yu A 2009 *J. Phys. D: Appl. Phys.* **42** 235208
[37] Meek J M and Craggs J D 1978 *Electrical Breakdown in Gases* (Chichester: Wiley)
[38] Penache M C 2002 *Study of High-Pressure Glow Discharges Generated by Micro-Structured Electrode (MSE) Arrays* (Ph. D. Dissertation) (Frankfurt am Main)
[39] Dakin T W, Gerhold J and Krasucki Z 1977 *Proceedings of the International Conference on Large High-Voltage Electric Systems,* 1977, Paris, p. 1
[40] Lisovskiy V A, Yakovin S D and Yegorenkov V D 2000 *J. Phys. D: Appl. Phys.* **33** 2722
[41] Sadiq Y, Kurt H Y, Albarzanji A O, Alekperov S D and Salamov B G 2009 *Solid-State Electron.* **53** 1009
[42] Sadiq Y, Kurt H Y and Salamov B G 2008 *J. Phys. D: Appl. Phys.* **41** 225204
[43] Gao F, Li X C, Zhao S X and Wang Y N 2012 *Chin. Phys. B* **21** 075203